

# Cross-Sectional and Longitudinal Comparison of Tau Imaging with $^{18}\text{F}$ -MK6240 and $^{18}\text{F}$ -Flortaucipir in Populations Matched for Age, MMSE and Brain Beta-Amyloid Burden

P. Bourgeat<sup>1</sup>, N. Krishnadas<sup>2,3</sup>, V. Doré<sup>2,4</sup>, R. Mulligan<sup>2</sup>, R. Tyrrell<sup>2</sup>, S. Bozinovski<sup>2</sup>, K. Huang<sup>2</sup>, J. Fripp<sup>1</sup>, V.L. Villemagne<sup>6</sup>, C.C. Rowe<sup>2,5</sup> for the Alzheimer's Disease Neuroimaging Initiative\* and the AIBL research group

1. Australian e-Health Research Centre, CSIRO, Brisbane, QLD, Australia; 2. Austin Health, Melbourne, VIC, Australia; 3. Florey Institute of Neurosciences & Mental Health, Parkville, VIC, Australia; 4. Australian e-Health Research Centre, CSIRO, Melbourne, VIC, Australia; 5. The University of Melbourne, Melbourne, VIC, Australia; 6. University of Pittsburgh, Pittsburgh, PA, 15260, USA

Corresponding Author: Pierrick Bourgeat, The Australian e-Health Research Centre, CSIRO, Level 7, 296 Herston Road, Herston Qld 4029, Australia, Tel: 07 3253 3659, [Pierrick.bourgeat@csiro.au](mailto:Pierrick.bourgeat@csiro.au)

## Abstract

**OBJECTIVES:** Longitudinal tau quantification may provide a useful marker of drug efficacy in clinical trials. Different tau PET tracers may have different sensitivity to longitudinal changes, but without a head-to-head dataset or a carefully designed case-matching procedure, comparing results in different cohorts can be biased. In this study, we compared the tau PET tracers,  $^{18}\text{F}$ -MK6240 and  $^{18}\text{F}$ -flortaucipir (FTP), both cross-sectionally and longitudinally by case-matching subjects in the AIBL and ADNI longitudinal cohort studies.

**METHODS:** A subset of 113 participants from AIBL and 113 from ADNI imaged using  $^{18}\text{F}$ -MK6240 and  $^{18}\text{F}$ -FTP respectively, with baseline and follow-up, were matched based on baseline clinical diagnosis, MMSE, age and amyloid ( $\text{A}\beta$ ) PET centiloid value. Subjects were grouped as 64  $\text{A}\beta^-$  cognitively unimpaired (CU), 22  $\text{A}\beta^+$  CU, 14  $\text{A}\beta^+$  mild cognitive impairment (MCI) and 13  $\text{A}\beta^+$  Alzheimer's disease (AD). Tracer retention was measured in the mesial, temporoparietal, rest of the cortex, and a meta-temporal region composed of entorhinal, inferior/middle temporal, fusiform, parahippocampus and amygdala. T-tests were employed to assess group separation at baseline using SUVR Z-scores and longitudinally using  $\text{SUVR}\%/\text{Yr}$ .

**RESULTS:** Both tracers detected statistically significant differences at baseline in most regions between all clinical groups. Only  $^{18}\text{F}$ -MK6240 showed statistically significant higher rate of SUVR increase in  $\text{A}\beta^+$  CU compared to  $\text{A}\beta^-$  CU in the mesial, meta-temporal and temporoparietal regions.

**CONCLUSION:**  $^{18}\text{F}$ -MK6240 appears to be a more sensitive tracer for change in tau level at the preclinical stage of AD.

**Key words:**  $^{18}\text{F}$ -MK6240,  $^{18}\text{F}$ -flortaucipir, tau PET.

## Introduction

Alzheimer's disease is characterised by the deposition of extracellular  $\beta$ -amyloid plaques ( $\text{A}\beta$ ) and intracellular neurofibrillary tangles (tau). Several PET tracers allow the in-vivo quantification of tau. While the cross-sectional analysis of these tracers

for early detection of tau has been widely studied, their longitudinal analysis is limited. Longitudinal tau quantification may provide a useful marker of anti-tau drug efficacy in clinical trials, and different tau PET tracers may provide different sensitivity to longitudinal changes, but without a head-to-head dataset or a carefully designed case-matching procedure, comparing results in different cohorts can be biased. In this study, we aim to minimise this bias by matching subjects in two cohorts imaged using  $^{18}\text{F}$ -MK6240 and  $^{18}\text{F}$ -flortaucipir.

A recent direct comparison of  $^{18}\text{F}$ -flortaucipir and  $^{18}\text{F}$ -MK6240 (1) showed that both tracers detect tau in common regions that are typically associated with tau pathology in AD. They also showed a good SUVR correlation in these regions. This analysis also revealed that  $^{18}\text{F}$ -MK6240 exhibited a greater dynamic range, with the author concluding that this could lead to an earlier detection of tau accumulation in longitudinal studies, but direct longitudinal comparison would be required to support these findings.

There has been a number of longitudinal studies for  $^{18}\text{F}$ -Flortaucipir looking at the accumulation in cognitively unimpaired (CU) (2), CU/mild cognitive impairment (MCI) (3, 4), MCI (5) and a mix of CU, MCI and Alzheimer's disease (AD) (6–8). Other studies have also looked at the pattern of accumulation in clinical variants of AD (9) and autosomal AD (10). While most studies find statistically significantly higher rates of tau accumulation at the prodromal stage of the disease, the results at the preclinical stage are mixed, with only 2 studies (3, 11) finding statistically significantly higher rates of tau accumulation in the  $\text{A}\beta$  positive CU compared with the  $\text{A}\beta$  negative CU.

Given that  $^{18}\text{F}$ -MK6240 is a more recent tracer, longitudinal studies using this tracer are more sparse, with only two studies looking at the pattern of longitudinal accumulation in CU, MCI and AD (12, 13). Both studies showed that  $^{18}\text{F}$ -MK6240 could detect statistically significant tau accumulation in both

preclinical and prodromal AD subjects.

Given the interest in using tau imaging in clinical trials, it is becoming increasingly important to compare the various tau tracers in closely matched populations to properly evaluate their ability to measure longitudinal changes. While there is no direct longitudinal comparison of  $^{18}\text{F}$ -Flortaucipir and  $^{18}\text{F}$ -MK6240, we have case-matched two independent populations based on clinical diagnosis, Centiloid value, Mini Mental State Examination (MMSE) score and age.

## Methods

Data were obtained from both the Australian Imaging Biomarkers and Lifestyle study (AIBL) and the ADNI database ([adni.loni.usc.edu](https://adni.loni.usc.edu)). The ADNI was launched in 2003 as a public-private partnership by the National Institute on Aging, the Food and Drug Administration, private pharmaceutical companies and non-profit organizations. Its primary goal was to test whether neuroimaging like serial magnetic resonance imaging (MRI), PET, biological markers, and clinical and neuropsychological assessment can be combined to measure the progression of MCI and early AD. A detailed description of the inclusion criteria can be found on the ADNI website ([www.adni-info.org](http://www.adni-info.org)). Data were downloaded from the ADNI database ([adni.loni.usc.edu](https://adni.loni.usc.edu)).

This study was approved by the Austin Health Human Research Ethics Committee (HREC/18/Austin/201). All AIBL participants gave written consent for publication of de-identified data. All ADNI participants signed written informed consent for participation in the ADNI, as approved by the institutional board at each participating centre.

## Participants

136 participants from the AIBL study imaged using  $^{18}\text{F}$ -MK6240 at baseline and follow-up and 273 participants from the ADNI study imaged using  $^{18}\text{F}$ -Flortaucipir at baseline and follow-up were considered for this study. To ensure that the two datasets were as comparable as possible, participants were excluded from the analysis if a different scanner was used for the baseline and follow-up tau-PET scans or the delay between baseline and follow-up was less than 10 months or more than 30 months. They were also excluded if an amyloid ( $\text{A}\beta$ ) PET scan was not available within 1 year of the baseline tau PET scan, if MMSE at baseline was not available, or if either baseline or follow-up clinical diagnosis was not either CU, MCI or AD. Furthermore, we also excluded participants who were cognitively impaired but were amyloid negative.

$^{18}\text{F}$ -MK6240 acquisitions were performed using two scanners (Philips Gemini TF64 and Siemens Biograph 128 mCT) while  $^{18}\text{F}$ -FTP acquisitions were performed using 23 different scanner models. Acquisition details for  $^{18}\text{F}$ -MK6240 have been previously described (12) and

details for the  $^{18}\text{F}$ -FTP acquisition are available on the ADNI website (<https://adni.loni.usc.edu/methods/pet-acquisition>).

## PET Analysis

Both  $^{18}\text{F}$ -NAV4694  $\text{A}\beta$  PET and  $^{18}\text{F}$ -MK6240 tau PET images from the AIBL study were smoothed to a uniform 8mm FWHM resolution following the ADNI pre-processing pipeline (14), so they would match the resolution of the pre-processed  $^{18}\text{F}$ -Flortaucipir,  $^{18}\text{F}$ -Florbetapir and  $^{18}\text{F}$ -Florbetaben scans downloaded from ADNI.

All PET images were then analysed using CapAIBL, a PET-only quantification method (15). The  $\text{A}\beta$  PET scans ( $^{18}\text{F}$ -NAV4694 for AIBL and either  $^{18}\text{F}$ -Florbetapir or  $^{18}\text{F}$ -Florbetaben for ADNI) were quantified using Centiloids (CL) using our recently reported Non-negative Matrix Factorisation quantification method (16, 17). Amyloid positivity ( $\text{A}\beta^+/\text{A}\beta^-$ ) was defined based on a threshold of 25CL. Subjects were grouped as cognitively unimpaired amyloid negative ( $\text{A}\beta^-$  CU),  $\text{A}\beta^+$  CU, mild cognitive impairment amyloid positive ( $\text{A}\beta^+$  MCI) and Alzheimer's disease amyloid positive ( $\text{A}\beta^+$  AD).

The tau PET scans ( $^{18}\text{F}$ -MK6240 for AIBL and  $^{18}\text{F}$ -Flortaucipir for ADNI) were spatially normalised using the CapAIBL PCA based approach (18) and the cerebellum cortex was used as the reference region to compute the Standardised Uptake Value Ratio (SUVR). Tracer retention was measured in four regions: the mesial (Me), temporoparietal (Te) and rest of the cortex (R) (19) as well as metatemporal region (MT) composed of entorhinal, inferior/middle temporal, fusiform, parahippocampus and amygdala (3). CapAIBL was also used to generate mean surface projection of Tau tracer uptake for each clinical group. To facilitate the interpretation of the results, the surface projections were mirrored and averaged to remove any asymmetry in the datasets which, given the recent head-to-head comparison results (1), are likely participant specific and not representative of the binding properties of the tracer.

No correction for partial volume effect was conducted for either amyloid or tau quantification.

## Statistical Analysis

SUVR were transformed into Z-scores for the cross-sectional analysis, and the percentage annual change ( $\text{SUVR\%/Year}$ ) was used for the longitudinal analysis and was defined as the annualized difference in SUVR between baseline and follow-up, normalized by the baseline SUVR. T-tests were employed to assess group separation at baseline using the SUVR Z-score and longitudinally using  $\text{SUVR\%/Year}$ . No correction for multiple comparisons was conducted. A power analysis with 80% power and  $\alpha = 0.05$  was also conducted to estimate the number of participants needed to detect a

25% annualized reduction of Tau accumulation in A $\beta$ + CU for both tau tracers. A 10000 bootstrap sampling was conducted to estimate the 95% confidence intervals.

## Populations matching

The two populations were matched in terms of age, Centiloid and MMSE within each of the four groups (A $\beta$ - CU, A $\beta$ + CU, A $\beta$ + MCI and A $\beta$ + AD). The age, Centiloids and MMSE of each participant were first transformed into Z-scores, using the combined A $\beta$ - CU from both AIBL and ADNI as reference population. For each baseline participant scanned using  $^{18}\text{F}$ -MK6240, a weighted distance was computed with all baseline participant scanned using  $^{18}\text{F}$ -FTP sharing the same clinical group. The weighted distance D was defined as follows:

$$D = \frac{\alpha * |Z(\text{Age}_{\text{MK}}) - Z(\text{Age}_{\text{FTP}})| + \beta * |Z(\text{CL}_{\text{MK}}) - Z(\text{CL}_{\text{FTP}})| + \gamma * |Z(\text{MMSE}_{\text{MK}}) - Z(\text{MMSE}_{\text{FTP}})|}{\alpha + \beta + \gamma}$$

With the Z() function denoting the Z-score, and  $\alpha$ ,  $\beta$  and  $\gamma$  representing the weight assigned to each Z-score variables. For each  $^{18}\text{F}$ -MK6240 baseline scan, the  $^{18}\text{F}$ -FTP baseline scan within the same diagnostic group and with the shortest distance D was selected as the best matching candidate. To ensure that the matched scans were as similar as possible, we established a threshold T to define a maximum allowable distance. For any given  $^{18}\text{F}$ -MK6240 baseline scan, if the most similar  $^{18}\text{F}$ -FTP scan had a distance D greater than T, the  $^{18}\text{F}$ -MK6240 is deemed to be unmatchable given the available  $^{18}\text{F}$ -FTP scans available and is excluded. To ensure that the interval between baseline and follow-up were comparable between both studies, the matched  $^{18}\text{F}$ -FTP scan was also excluded if the interval between baseline and follow-up was 6 months longer or shorter than that of the matched  $^{18}\text{F}$ -MK6240. The procedure was run until all the baseline  $^{18}\text{F}$ -MK6240 scans were either matched with a suitable  $^{18}\text{F}$ -FTP scan or excluded. In our experiments, we used the weights ( $\alpha=1$ ,  $\beta=1$ ,  $\gamma=2$ ) and a threshold T=0.5 which corresponds to half a standard deviation of difference across all three metrics.

## Results

### Matched populations

At the end of the matching procedure, 114 pairs of participants were matched, including 65 A $\beta$ - CU, 22 A $\beta$ + CU, 14 A $\beta$ + MCI and 13 A $\beta$ + AD. One of the matched  $^{18}\text{F}$ -FTP A $\beta$ - CU participant had high uptake in the MT and Te (Z-Score >7). The scan was visually read as being positive and was deemed to be an outlier. It was therefore excluded from all further analysis along with its matched  $^{18}\text{F}$ -MK6240 A $\beta$ - CU participant. As a results, 113 pairs of participants remained, including 64 A $\beta$ - CU. As per design, there was no statistically significant difference in MMSE, age, Centiloid and number of years between baseline and follow-up at baseline between the  $^{18}\text{F}$ -

MK6240 and  $^{18}\text{F}$ -FTP participant within each of the four diagnosis groups (Table 1). There was also no difference in CDR Sum of Boxes, ApoE status or gender between the two tracers in each group. The  $^{18}\text{F}$ -FTP participants were however more educated in all diagnosis groups compared to their matched  $^{18}\text{F}$ -MK6240.

### Cross sectional analysis

Using the 113 pairs of matched participants, regional SUVR at baseline for both tracers were transformed into Z-scores using each tracer's respective A $\beta$ - CU population as reference. Surface projections of the mean SUVR images for the A $\beta$ - CU at baseline and follow-up are presented in supplementary Figure 1. The Z-scores were then compared between each pair of diagnosis groups using t-test (Figure 1.a). The corresponding effect sizes are presented in Table 2.

Baseline SUVR Z-scores were statistically significantly different between each group in all regions, except for A $\beta$ - CU and A $\beta$ + in the R region (excludes Me and Te) of the cortex with both tracers.

When comparing A $\beta$ - CU to A $\beta$ + CU, both tracers showed statistically significant differences in the Me and MT. However, better group separation was obtained when using  $^{18}\text{F}$ -MK6240, with a higher effect size in both the Me ( $\text{ES}_{\text{MK6240}}=1.15$ ,  $\text{ES}_{\text{FTP}}=0.87$ ) and MT ( $\text{ES}_{\text{MK6240}}=1.11$ ,  $\text{ES}_{\text{FTP}}=0.89$ ). We also observed that the SUVR Z-Scores were typically higher using  $^{18}\text{F}$ -MK6240 compared to using  $^{18}\text{F}$ -FTP, especially in A $\beta$ + MCI and A $\beta$ + AD.

Surface projections of mean SUVR Z-Scores in each subgroup for  $^{18}\text{F}$ -MK6240 and  $^{18}\text{F}$ -FTP are presented in Figure 2.a. These projections illustrate similar patterns of retention with both tracers, starting in the Me before spreading to the Te and eventually to the rest of the cortex.

### Longitudinal analysis

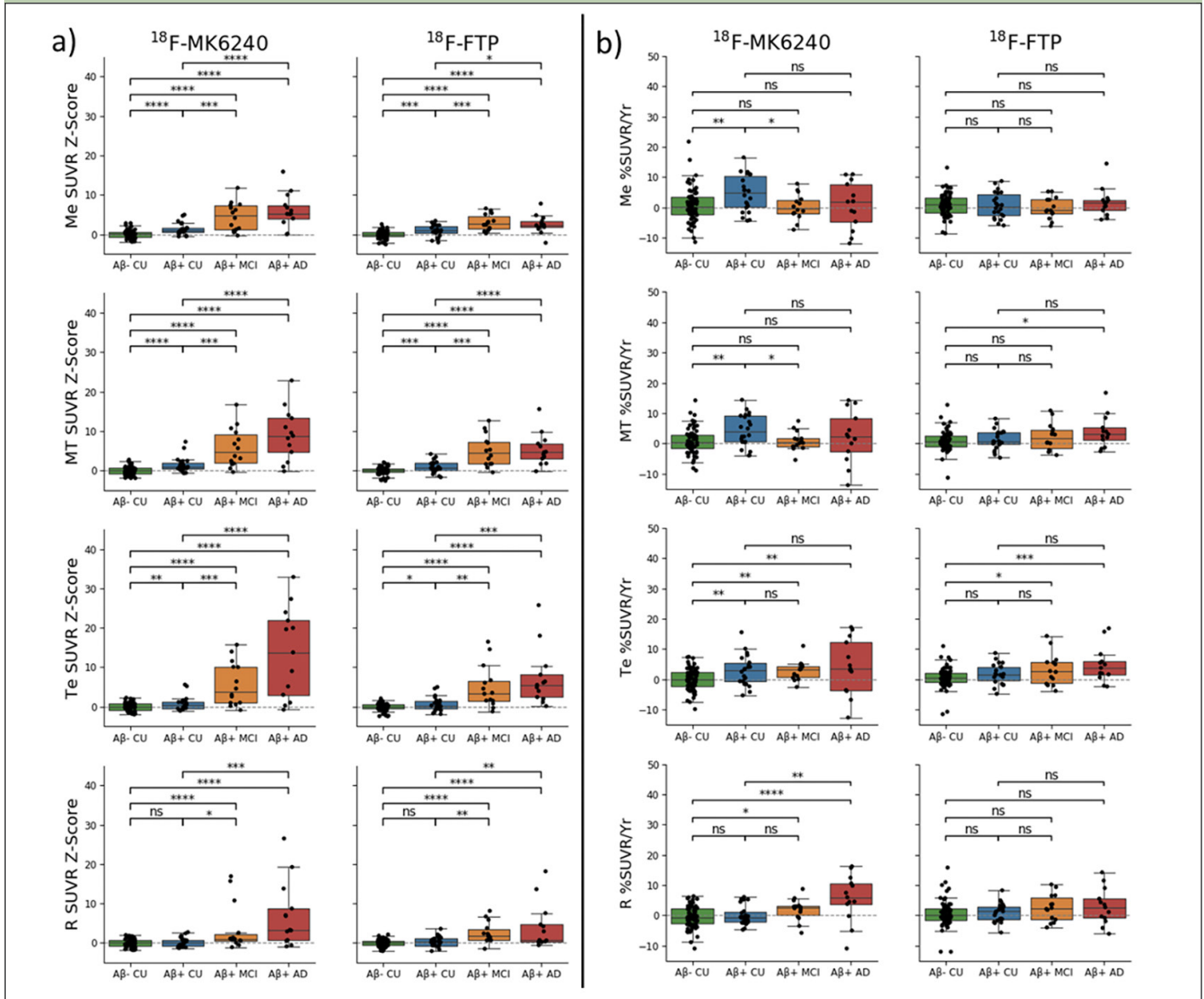
For each tracer, the 113 baseline/follow-up pairs were used to compute the rate of change, expressed in SUVR%/Year. Using the classification at baseline, the rates were compared between A $\beta$ - CU and A $\beta$ + CU/MCI/AD as well as A $\beta$ + CU and A $\beta$ + MCI/AD using t-test (Figure 1.b). The corresponding effect sizes are presented in Table 2.

The rate of SUVR change in A $\beta$ + CU was statistically significantly higher than that of A $\beta$ - CU in the Me, MT and Te when using  $^{18}\text{F}$ -MK6240. No differences between A $\beta$ - and A $\beta$ + CU were observed with  $^{18}\text{F}$ -FTP. The rate of SUVR change in A $\beta$ + MCI and AD was statistically significantly higher than that of A $\beta$ - CU in the Te and R when using  $^{18}\text{F}$ -MK6240, and in the Te with  $^{18}\text{F}$ -FTP, but also in the MT for the A $\beta$ + AD group.

With  $^{18}\text{F}$ -MK6240, the rate of SUVR change in the A $\beta$ + MCI was statistically significantly smaller than that of A $\beta$ + CU in the Me and MT. No differences between



**Figure 1.** (a) Baseline SUVR Z-Scores and (b) percentage of SUVR change (SUVR%/Year) for  $^{18}\text{F}$ -MK6240 and  $^{18}\text{F}$ -FTP in the four regions of interest: mesial (Me), metatemporal (MT), temporoparietal (Te) and rest of the cortex (R). (ns: not significant. \*:  $p < 0.05$ ; \*\*:  $p < 0.01$ ; \*\*\*:  $p < 0.001$ ; \*\*\*\*:  $p < 0.0001$ ). By definition the mean  $\text{A}\beta^-$  CU Z-score is zero in all area



$\text{A}\beta^+$  CU and  $\text{A}\beta^+$  MCI were observed with  $^{18}\text{F}$ -FTP. The rate of SUVR change in the  $\text{A}\beta^+$  AD was statistically significantly higher than the rate in the  $\text{A}\beta^+$  CU in the R with  $^{18}\text{F}$ -MK6240. No differences between  $\text{A}\beta^+$  CU and  $\text{A}\beta^+$  AD were observed with  $^{18}\text{F}$ -FTP.

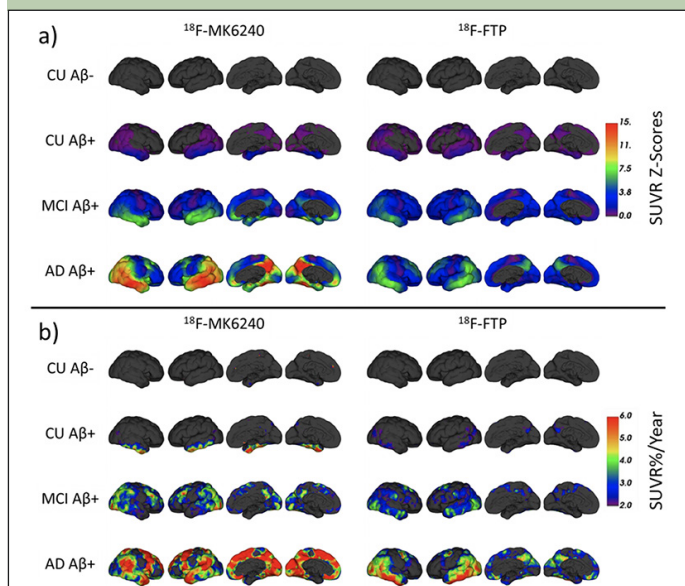
We also observed a few AD subjects with large negative rates of accumulation when using  $^{18}\text{F}$ -MK6240, which is consistent with a previous report (12) and is likely driven by instability in the reference region in this cohort.

Surface projections of mean SUVR%/Year in each subgroup for  $^{18}\text{F}$ -MK6240 and  $^{18}\text{F}$ -FTP are presented in Figure 2.b. These show early accumulation in the  $\text{A}\beta^+$  CU in the Me which is not visible when using  $^{18}\text{F}$ -FTP. In the  $\text{A}\beta^+$  MCI, with  $^{18}\text{F}$ -MK6240, the increase was the strongest in the posterior part of the temporal, the occipital lobe as well as the superior frontal. With  $^{18}\text{F}$ -FTP,

the inferior temporal and occipital showed the strongest increase. In the  $\text{A}\beta^+$  AD,  $^{18}\text{F}$ -MK6240 showed the largest increase in the temporal pole, parietal, occipital, superior frontal and precuneus. With  $^{18}\text{F}$ -FTP, the inferior temporal and occipital showed the strongest increase, with also noticeable increase in the parietal, superior frontal and precuneus.

We also conducted a power analysis to estimate the number of  $\text{A}\beta^+$  CU participants required to detect a 25% reduction in annual change of SUVR in a 2-arm placebo-controlled trial (Table 23). This shows that in the regions of early tau deposition (Me, MT), the number of participants required to detect a 25% reduction in annual change of SUVR using  $^{18}\text{F}$ -MK6240 would be almost an order of magnitude smaller than the number required when using  $^{18}\text{F}$ -FTP.

**Figure 2.** (a) Mean SUVR Z-Scores at baseline and (b) mean increase in SUVR%/Year in each subgroup for  $^{18}\text{F}$ -MK6240 (Left) and  $^{18}\text{F}$ -FTP (Right)



## Discussion

In this paper, we have compared the first-generation tau tracer  $^{18}\text{F}$ -Flortaucipir to the more recently developed tau tracer  $^{18}\text{F}$ -MK6240, both cross-sectionally and longitudinally. Since no longitudinal head-to-head dataset is currently available, we matched two independent datasets from AIBL and ADNI, by minimizing the difference in MMSE, Centiloid and age at baseline. Our matching procedure was able to identify 113 pairs of participants who had no significant difference at baseline between those three metrics within any of the diagnosis groups, and no difference in the number of years between the acquisition of the baseline and follow-up scans.

Since there are no published transforms to compare SUVR between  $^{18}\text{F}$ -FTP and  $^{18}\text{F}$ -MK6240, we opted to convert the SUVRs into Z-Scores, an approach similar

to CenTauRz which we have previously proposed to compare the different tau tracers using unpaired datasets (20). The cross-sectional analysis showed that both tracers were able to identify statistically significant differences at baseline between each diagnostic group. It also showed that the dynamic range of  $^{18}\text{F}$ -MK6240 was generally larger than that observed with  $^{18}\text{F}$ -FTP, in agreement with the direct head-to-head comparison of (1) which showed that the SUVR dynamic range of  $^{18}\text{F}$ -MK6240 was almost 2-folds greater than that of  $^{18}\text{F}$ -FTP. While both  $^{18}\text{F}$ -MK6240 and  $^{18}\text{F}$ -FTP could identify statistically significant differences between Aβ- CU to Aβ+ CU, the group separation was much larger when using  $^{18}\text{F}$ -MK6240. This would indicate that  $^{18}\text{F}$ -MK6240 might be able to better detect early tau accumulation.

The longitudinal analysis also showed that  $^{18}\text{F}$ -MK6240 could detect a statistically significant increase in the rate of tau accumulation in the Aβ+ CU compared to the Aβ- CU in both the mesial and metatemporal, which could not be detected using  $^{18}\text{F}$ -FTP in our matched cohort. It is possible that the lack of statistically significant difference in the rate of accumulation in the Aβ+ CU with  $^{18}\text{F}$ -FTP could be driven by the selected population as previous work has shown statistically significant difference between these groups in ADNI scans (11), although those differences were limited to the temporal inferior region, which could be diluted in our larger composite regions. Other groups using similar composite region, but in different cohorts, had mixed findings with either statistically significant difference found (3) or no difference (8). Recent work from Knopman and colleagues (2) showed that the rate of tau increase detected using  $^{18}\text{F}$ -FTP was much higher in subjects with high Aβ load, and this could explain differences between studies if their respective distribution of Aβ load at baseline is significantly different. One strength of our study is that both tracers were matched for Centiloid at baseline, which should minimize difference in tau accumulation due to differences in Aβ load.

Using  $^{18}\text{F}$ -MK6240, the rate of SUVR increase was statistically significantly smaller in the mesial from

**Table 1.** Mean (Standard deviation) of MMSE, centiloid, age, number of years between baseline and follow-up scans, CDR SOB, years of education as well as % of female and ApoE E4 for the baseline  $^{18}\text{F}$ -MK6240 and  $^{18}\text{F}$ -FTP and the corresponding p value

	Aβ- CU			Aβ+ CU			Aβ+ MCI			Aβ+ AD		
	$^{18}\text{F}$ -MK6240	$^{18}\text{F}$ -FTP	p value	$^{18}\text{F}$ -MK6240	$^{18}\text{F}$ -FTP	p value	$^{18}\text{F}$ -MK6240	$^{18}\text{F}$ -FTP	p value	$^{18}\text{F}$ -MK6240	$^{18}\text{F}$ -FTP	p value
MMSE	28.6(1.2)	28.9(1.1)	0.248	28.0(1.6)	28.3(1.5)	0.504	26.4(1.2)	26.6(1.1)	0.627	22.7(3.0)	22.8(3.2)	0.95
Centiloid	1.3(8.3)	2.4(9.6)	0.491	61.5(29.1)	63.0(30.1)	0.872	97.4(39.9)	87.4(30.2)	0.461	95.0(30.6)	90.9(22.6)	0.701
Age	74.1(4.4)	73.1(6.3)	0.319	76.7(6.2)	75.8(5.5)	0.618	76.6(6.9)	76.2(7.0)	0.894	71.8(8.6)	73.8(8.4)	0.557
Tau interval (Years)	1.4(0.3)	1.4(0.4)	0.511	1.4(0.4)	1.4(0.4)	0.924	1.3(0.3)	1.2(0.4)	0.361	1.4(0.4)	1.2(0.5)	0.441
CDR SOB	0.1(0.2)	0.0(0.2)	0.625	0.2(0.4)	0.0(0.2)	0.106	1.5(1.1)	1.5(1.1)	0.866	4.8(1.8)	4.8(1.5)	0.954
Years of Education	14.8(3.0)	16.4(2.3)	<b>&lt;0.001</b>	13.5(3.1)	16.7(2.4)	<b>&lt;0.001</b>	14.0(2.9)	16.4(1.9)	<b>0.014</b>	12.8(2.9)	15.5(2.7)	<b>0.042</b>
Sex (% female)	48%	62%	0.219	55%	55%	1	50%	36%	0.703	46%	38%	1.000
ApoE (%E4)*	33%	33%	0.900	57%	52%	1	67%	71%	0.870	67%	91%	0.432

\* ApoE genotype was only available for 105  $^{18}\text{F}$ -MK6240 participants and 110  $^{18}\text{F}$ -FTP participants; Bold fonts indicate statistically significant differences.

**Table 2.** Effect size at baseline (SUVR) and using the percentage rate of SUVR increase (%SUVR/Year ) between the different clinical groups using  $^{18}\text{F}$ -MK6240 or  $^{18}\text{F}$ -FTP in the four regions of interest: mesial (Me), metatemporal (MT), temporoparietal (Te) and rest of the cortex (R)

Effect Size	ROI	Baseline SUVR		Longitudinal SUVR%/Year	
		$^{18}\text{F}$ -MK6240	$^{18}\text{F}$ -FTP	$^{18}\text{F}$ -MK6240	$^{18}\text{F}$ -FTP
A $\beta$ - CU vs A $\beta$ + CU	Me	1.15	0.87	0.68	0.01
	MT	1.11	0.89	0.79	0.19
	Te	0.68	0.62	0.76	0.36
	R	0.2	0.34	0.14	0.09
A $\beta$ - CU vs A $\beta$ + MCI	Me	2.72	2.62	0.12 0.11	0.19
	MT	2.74	2.83	0.01	0.38
	Te	2.43	2.24	0.86 0.87	0.73
	R	1.43	1.93	0.66	0.43
A $\beta$ - CU vs A $\beta$ + AD	Me	3.29	2.10	0.02	0.24
	MT	3.47	3.06	0.29	0.81
	Te	3.13	2.60	0.9	1.12
	R	2.17	1.76	1.43	0.51

**Table 3.** Mean (Standard deviation) increase in SUVR/Year for  $^{18}\text{F}$ -MK6240 and  $^{18}\text{F}$ -FTP in the A $\beta$ + CU, and the corresponding sample size estimates (95% confidence intervals based on bootstrapping) to detect a 25% reduction in the rate of tau accumulation after 1 year using the mesial (Me), metatemporal (MT) and temporoparietal (Te) regions

ROI	$^{18}\text{F}$ -MK6240 A $\beta$ + CU		$^{18}\text{F}$ -FTP A $\beta$ + CU	
	Mean (SD) change in SUVR/Year	N per arm (95% CI)	Mean (SD) change in SUVR/Year	N per arm (95% CI)
Me	0.052 (0.071)	464 (170 - 2055)	0.006 (0.051)	20121 (718 - >10000)
MT	0.051 (0.065)	406 (148 - 1680)	0.016 (0.039)	1507 (309 - >10000)
Te	0.036 (0.061)	736 (273 - 5378)	0.023 (0.043)	897 (271- >10000)

A $\beta$ + MCI compared to the rates from A $\beta$ + CU, while significantly larger in the rest of the cortex in A $\beta$ + MCI/AD compared to A $\beta$ + CU. This pattern follows the expected sequence of Tau deposition, with Tau deposition expected to start in the mesial, spreading to inferior and middle temporal gyri (captured by the metatemporal mask) at the preclinical stages of the disease and reaching the rest of the cortex at the prodromal/symptomatic stage of the disease. While a similar trend was observed with  $^{18}\text{F}$ -FTP, it failed to reach statistical significance.

The spatial pattern of  $^{18}\text{F}$ -MK6240 increase was quite different to the pattern obtained using  $^{18}\text{F}$ -FTP, especially in the A $\beta$ + cognitively impaired groups. Our results indicate that  $^{18}\text{F}$ -MK6240 is a more sensitive tracer than  $^{18}\text{F}$ -FTP, which is consistent with a previous head-to-head comparison showing  $^{18}\text{F}$ -MK6240 having lower non-specific binding than  $^{18}\text{F}$ -FTP (1,21). Furthermore, in vitro studies showed  $^{18}\text{F}$ -MK6240 has higher affinity for paired helical filament tau than  $^{18}\text{F}$ -FTP (22). A higher affinity for tau and a lower non-specific PET signal likely allows  $^{18}\text{F}$ -MK6240 to detect earlier and more extensive tau deposition in the brain.

The estimated sample sizes required to detect a 25% reduction in annual change of SUVR were much lower when using  $^{18}\text{F}$ -MK6240 compared to  $^{18}\text{F}$ -FTP. With  $^{18}\text{F}$ -

MK6240, the number were similar for both the mesial, metatemporal and temporoparietal, whereas  $^{18}\text{F}$ -FTP had much higher number for the mesial, likely reflecting the lack of binding in the hippocampus with this tracer compounded by spillover from non-specific off-target binding in the choroid plexus. These results indicate that  $^{18}\text{F}$ -MK6240 might be better suited than  $^{18}\text{F}$ -FTP for anti-A $\beta$  and/or anti-tau clinical trials in the early stages of AD.

The main limitation of this paper is that we are using case-matched rather than true head-to-head data, and while we have taken many steps to reduce the potential differences between the datasets, we cannot account for other differences that might contribute to some of the differences observed in the results. For instance, 23 different scanners were used for the acquisitions of  $^{18}\text{F}$ -FTP compared to two for  $^{18}\text{F}$ -MK6240 which may increase the variance in the  $^{18}\text{F}$ -FTP measurements. A true head-to-head study, similar to the head-to-head scans acquired for the Centiloid study will be required to confirm those findings.

We also did not take into account possible effects of off-target binding in the meninges spilling into the target regions. While a comparison at baseline showed statistically significant differences in meningeal SUVR between clinical groups in  $^{18}\text{F}$ -MK6240, with A $\beta$ + MCI/



AD showing higher meningeal SUVR compared to the CU groups (supplementary Figure 2), there was no difference in their rate of change in any of the groups, and those were not statistically significantly different from 0 (supplementary Figure 3). This is consistent with a recent study reporting that the extracerebral uptake was stable over one year (23). Therefore, while  $^{18}\text{F}$ -MK6240 retention in the meninges might contribute to some of the differences observed at baseline, it was unlikely to contribute to the groups difference observed in our longitudinal analysis.

We also did not consider different reference regions for the two tracers. While some recent work has been looking at the best reference region for  $^{18}\text{F}$ -FTP to detect longitudinal changes (6, 11, 24), results using  $^{18}\text{F}$ -MK6240 are still limited (12) and require further evaluation. Therefore, we only selected a single reference region that has been frequently used in previous work for both tracers. However, future work in this area is warranted.

Lastly, we did not include partial volume correction (PVC). However, since both tracers were quantified the same way, we do not expect PVC to change the overall conclusions.

## Conclusions

We have proposed a framework to match two Tau tracers acquired in two independent studies. The cross-sectional and longitudinal analysis revealed that  $^{18}\text{F}$ -MK6240 might be better suited to detect early Tau accumulation and be a better tracer to be used in preclinical trials. While our framework tried to minimise difference between the two populations, head-to-head longitudinal comparison will be required to confirm these results.

\* Data used in preparation of this article were obtained from the Alzheimer's Disease Neuroimaging Initiative (ADNI) database (adni.loni.usc.edu). As such, the investigators within the ADNI contributed to the design and implementation of ADNI and/or provided data but did not participate in analysis or writing of this report. A complete listing of ADNI investigators can be found at: [http://adni.loni.usc.edu/wp-content/uploads/how\\_to\\_apply/ADNI\\_Acknowledgement\\_List.pdf](http://adni.loni.usc.edu/wp-content/uploads/how_to_apply/ADNI_Acknowledgement_List.pdf)

**Acknowledgments:** Some of the data used in the preparation of this article were obtained from the Australian Imaging Biomarkers and Lifestyle flagship study of aging (AIBL), funded by the Commonwealth Scientific and Industrial Research Organization (CSIRO), National Health and Medical Research Council (NHMRC), and participating institutions. AIBL researchers are listed at [www.aibl.csiro.au](http://www.aibl.csiro.au). The authors thank all participants who took part in the study, as well as their families. The research was supported by the Australian Federal Government through NHMRC grants APP1132604 and APP1140853. Some of the data collection and sharing for this project was funded by the Alzheimer's Disease Neuroimaging Initiative (ADNI) (National Institutes of Health Grant U01 AG024904) and DOD ADNI (Department of Defense award number W81XWH-12-2-0012). ADNI is funded by the National Institute on Aging, the National Institute of Biomedical Imaging and Bioengineering, and through generous contributions from the following: AbbVie, Alzheimer's Association; Alzheimer's Drug Discovery Foundation; Araclon Biotech; BioClinica, Inc.; Biogen; Bristol-Myers Squibb Company; CereSpir, Inc.; Cogstate; Eisai Inc.; Elan Pharmaceuticals, Inc.; Eli Lilly and Company; EuroImmun; F. Hoffmann-La Roche Ltd and its affiliated company Genentech, Inc.; Fujirebio; GE Healthcare; IXICO Ltd.; Janssen Alzheimer Immunotherapy Research & Development, LLC.; Johnson & Johnson Pharmaceutical Research & Development LLC.; Lumosity; Lundbeck; Merck & Co., Inc.; Meso Scale Diagnostics, LLC.; NeuroRx Research; Neurotrack Technologies; Novartis Pharmaceuticals Corporation; Pfizer Inc.; Piramal Imaging; Servier; Takeda Pharmaceutical Company; and Transition Therapeutics. The Canadian

Institutes of Health Research is providing funds to support ADNI clinical sites in Canada. Private sector contributions are facilitated by the Foundation for the National Institutes of Health ([www.fnih.org](http://www.fnih.org)). The grantee organization is the Northern California Institute for Research and Education, and the study is coordinated by the Alzheimer's Therapeutic Research Institute at the University of Southern California. ADNI data are disseminated by the Laboratory for Neuro Imaging at the University of Southern California.

**Funding:** Cerveau provided a research grant to institution and materials for production of the PET tau tracer. Funding was also provided by the NHMRC of Australia (Grant numbers APP1132604, APP1140853, APP1152623). The sponsors had no role in the design and conduct of the study; in the collection, analysis, and interpretation of data or in the preparation of the manuscript but Cerveau did give approval for publication of the manuscript. Open access funding provided by CSIRO Library Services.

**Disclosure:** Christopher C. Rowe has received research grants from NHMRC, Enigma Australia, Biogen, Eisai, and Abbvie. He is on the scientific advisory board for Cerveau Technologies and consulted for Prothena, Eisai, Roche, and Biogen Australia. Victor Villemagne is and has been a consultant or paid speaker at sponsored conference sessions for Eli Lilly, Life Molecular Imaging, GE Healthcare, Abbvie, Lundbeck, Shanghai Green Valley Pharmaceutical Co Ltd, and Hoffmann La Roche. The other authors did not report any conflict of interest.

**Ethical standards:** All procedures performed in this study involving human participants were approved by and in accordance with the ethical standards of the Austin Health Human Research Ethics Committee (HREC/18/Austin/201). Informed consent was obtained from all participants.

**Open Access:** This article is distributed under the terms of the Creative Commons Attribution 4.0 International License (<http://creativecommons.org/licenses/by/4.0/>), which permits use, duplication, adaptation, distribution and reproduction in any medium or format, as long as you give appropriate credit to the original author(s) and the source, provide a link to the Creative Commons license and indicate if changes were made.

## References

- Gogola A, Minhas DS, Villemagne VL, et al. Direct comparison of the tau PET tracers [ $^{18}\text{F}$ ]flortaucipir and [ $^{18}\text{F}$ ]MK-6240 in human subjects. *J Nucl Med*. April 2021. <http://doi.org/10.2967/jnumed.120.254961>.
- Knopman DS, Lundt ES, Therneau TM, et al. Association of Initial  $\beta$ -Amyloid Levels With Subsequent Flortaucipir Positron Emission Tomography Changes in Persons Without Cognitive Impairment. *JAMA Neurol*. 2021;78:217-228. <http://doi.org/10.1001/jamaneurol.2020.3921>.
- Jack CR, Wiste HJ, Schwarz CG, et al. Longitudinal tau PET in ageing and Alzheimer's disease. *Brain J Neurol*. 2018;141:1517-1528. <http://doi.org/10.1093/brain/aww059>.
- Zhang R-Q, Chen S-D, Shen X-N, et al. Elevated Tau PET Signal Depends on Abnormal Amyloid Levels and Correlates with Cognitive Impairment in Elderly Persons without Dementia. *J Alzheimers Dis JAD*. 2020;78:395-404. <http://doi.org/10.3233/JAD-200526>.
- Xu G, Zheng S, Zhu Z, et al. Association of tau accumulation and atrophy in mild cognitive impairment: a longitudinal study. *Ann Nucl Med*. 2020;34:815-823. <http://doi.org/10.1007/s12149-020-01506-2>.
- Cho H, Choi JY, Lee HS, et al. Progressive tau accumulation in Alzheimer's disease: two-year follow-up study. *J Nucl Med*. March 2019. <http://doi.org/10.2967/jnumed.118.221697>.
- Pontecorvo MJ, Devous MD, Kennedy I, et al. A multicentre longitudinal study of flortaucipir ( $^{18}\text{F}$ ) in normal ageing, mild cognitive impairment and Alzheimer's disease dementia. *Brain J Neurol*. 2019;142:1723-1735. <http://doi.org/10.1093/brain/awz090>.
- Smith R, Strandberg O, Mattsson-Carlsson N, et al. The accumulation rate of tau aggregates is higher in females and younger amyloid-positive subjects. *Brain*. 2020;143:3805-3815. <http://doi.org/10.1093/brain/awaa327>.
- Phillips JS, Nitchie IV FJ, Da Re F, et al. Rates of longitudinal change in  $^{18}\text{F}$ -flortaucipir PET vary by brain region, cognitive impairment, and age in atypical Alzheimer's disease. *Alzheimers Dement*. 2022;18:1235-1247. <http://doi.org/10.1002/alz.12456>.
- Sanchez JS, Hanseeuw BJ, Lopera F, et al. Longitudinal amyloid and tau accumulation in autosomal dominant Alzheimer's disease: findings from the Colombia-Boston (COLBOS) biomarker study. *Alzheimers Res Ther*. 2021;13:27. <http://doi.org/10.1186/s13195-020-00765-5>.
- Young CB, Landau SM, Harrison TM, Poston KL, Mormino EC. Influence of common reference regions on regional tau patterns in cross-sectional and longitudinal [ $^{18}\text{F}$ ]-AV-1451 PET data. *NeuroImage*. 2021;243:118553. <http://doi.org/10.1016/j.neuroimage.2021.118553>.
- Krishnadas N, Doré V, Robertson J, et al. Rates of regional tau accumulation in ageing and across the Alzheimer's disease continuum: An AIBL  $^{18}\text{F}$ -

- MK6240 PET study. MedRxiv. March 2022:2022.03.11.22272240. <http://doi.org/10.1101/2022.03.11.22272240>.
13. Pascoal TA, Benedet AL, Tudorascu DL, et al. Longitudinal 18F-MK-6240 tau tangles accumulation follows Braak stages. *Brain J Neurol*. 2021;144:3517-3528. <http://doi.org/10.1093/brain/awab248>.
  14. Jagust WJ, Landau SM, Koeppe RA, et al. The Alzheimer's Disease Neuroimaging Initiative 2 PET Core: 2015. *Alzheimers Dement*. 2015;11:757-771. <http://doi.org/10.1016/j.jalz.2015.05.001>.
  15. Bourgeat P, Villemagne VL, Dore V, et al. Comparison of MR-less PiB SUVR quantification methods. *Neurobiol Aging*. 2015;36 Suppl 1:S159-166. <http://doi.org/10.1016/j.neurobiolaging.2014.04.033>.
  16. Bourgeat P, Doré V, Doecke J, et al. Non-negative matrix factorisation improves Centiloid robustness in longitudinal studies. *NeuroImage*. 2021;226:117593. <http://doi.org/10.1016/j.neuroimage.2020.117593>.
  17. Bourgeat P, Doré V, Burnham SC, et al.  $\beta$ -amyloid PET harmonisation across longitudinal studies: Application to AIBL, ADNI and OASIS3. *NeuroImage*. 2022;262:119527. <http://doi.org/10.1016/j.neuroimage.2022.119527>.
  18. Dore V, Bourgeat P, Burnham SC, et al. Automated reporting of tau quantification on the brain surface. *Alzheimers Dement J Alzheimers Assoc*. 2019;15:P1269. <http://doi.org/10.1016/j.jalz.2019.06.4811>.
  19. Villemagne VL, Dore V, Bourgeat P, et al. The Tau MeTeR composites for the generation of continuous and categorical measures of tau deposits in the brain. *J Mol Med Ther*. 2017;1:25-32.
  20. Dore V, Bullich S, Bohorquez SS, et al. CenTauRz: A standardized quantification of tau PET scans. *Alzheimers Dement*. 2022;18:e061177. <http://doi.org/10.1002/alz.061177>.
  21. Baker SL, Harrison TM, Maass A, La Joie R, Jagust WJ. Effect of Off-Target Binding on 18F-Flortaucipir Variability in Healthy Controls Across the Life Span. *J Nucl Med Off Publ Soc Nucl Med*. 2019;60:1444-1451. <http://doi.org/10.2967/jnumed.118.224113>.
  22. Hostetler ED, Walji AM, Zeng Z, et al. Preclinical Characterization of 18F-MK-6240, a Promising PET Tracer for In Vivo Quantification of Human Neurofibrillary Tangles. *J Nucl Med*. 2016;57:1599-1606. <http://doi.org/10.2967/jnumed.115.171678>.
  23. Fu JF, Lois C, Sanchez J, et al. Kinetic evaluation and assessment of longitudinal changes in reference region and extracerebral [18F] MK-6240 PET uptake. *J Cereb Blood Flow Metab Off J Int Soc Cereb Blood Flow Metab*. November 2022:271678X221142139. <http://doi.org/10.1177/0271678X221142139>.
  24. Schwarz CG, Therneau TM, Weigand SD, et al. Selecting software pipelines for change in flortaucipir SUVR: Balancing repeatability and group separation. *NeuroImage*. 2021;238:118259. <http://doi.org/10.1016/j.neuroimage.2021.118259>.

©The Authors 2023

How to cite this article: P. Bourgeat, N. Krishnadas, V. Doré, et al. Cross-Sectional and Longitudinal Comparison of Tau Imaging with <sup>18</sup>F-MK6240 and <sup>18</sup>F-Flortaucipir in Populations Matched for Age, MMSE and Brain Beta-Amyloid Burden. *J Prev Alz Dis* 2023;2(10):251-258; <http://dx.doi.org/10.14283/jpad.2023.17>